arXiv:cond-mat/0303189v1 [cond-mat.mtrl-sci] 11 Mar 2003

Temperature dependent total scattering structural study of $CaCu_3Ti_4O_{12}$

E. S. Božin,[1] V. Petkov,[2] P. W. Barnes,[3] P. M. Woodward,[3] T. Vogt,[4] S. D. Mahanti,[1] and S. J. L. Billinge[1]
[1]*Department of Physics and Astronomy and Center for Fundamental Materials Research, Michigan State University, Biomedical Physical Sciences, East Lansing, MI 48824-2320.*
[2]*Physics Department, Central Michigan University, Mount Pleasant, MI 48859.*
[3]*Department of Chemistry, Ohio State University, Columbus, OH 43210-1185.*
[4] *Physics Department, Brookhaven National Laboratory, Upton, NY 11973-5000.*
(Dated: March 22, 2022)

X-ray and neutron powder diffraction data as a function of temperature are analyzed for the colossal dielectric constant material $CaCu_3Ti_4O_{12}$. The local structure is studied using atomic pair distribution function analysis. No evidence is found for enhanced oxygen displacement parameters suggesting that short-range octahedral tilt disorder is minimal. However, an unusual temperature dependence for the atomic displacement parameters of calcium and copper is observed. Temperature dependent modeling of the structure, using bond valence concepts, suggests that the calcium atoms become underbonded below approximately 260 K, which provides a rationale for the unusually high Ca displacement parameters at low temperature.

PACS numbers: 61.10.-i,61.12-q,77.22.-d,77.84.-s

I. INTRODUCTION

Recently there has been considerable interest in the dielectric properties of the cubic perovskite-related $CaCu_3Ti_4O_{12}$ (CCTO). This material exhibits a giant dielectric constant response with a highly unusual temperature dependence. It has a high and relatively temperature independent low-frequency dielectric constant over a wide temperature range between 100 K and 600 K. However, below 100 K the value drops abruptly by almost three orders of magnitude, an effect that is not accompanied by a long-range structural phase transition.[1,2,3] The crystal structure of CCTO (s.g. $Im\overline{3}$)[4] is shown in Fig. 1. Its structure can be derived from the ideal cubic perovskite structure by superimposing a body centered ordering of Ca and Cu ions and a pronounced tilting of the titanium centered octahedra (tilt system $a^+a^+a^+$).[5] The tilting dramatically alters the coordination environments of the A-site cations, leading to a 4-coordinate square-planar environment for Cu and a 12-coordinate icosahedral environment for Ca. It is the mismatch in size and bonding preferences of these two ions and the titanium that drives the large octahedral tilting distortion. The system is an antiferromagnetic insulator below $T_N = 25$ K, as indicated by transport, neutron diffraction, and Raman studies.[1,2,6]

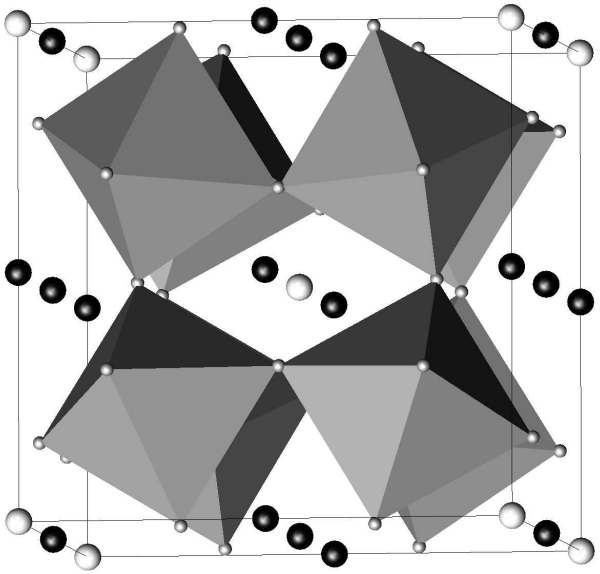


FIG. 1: $CaCu_3Ti_4O_{12}$ structure is cubic (space group $Im\overline{3}$): shown are TiO_6 octahedra, Ca atoms (large light spheres), and Cu atoms (dark spheres).

Numerous proposals have been put forward to uncover the origin of the giant dielectric response in CCTO, including both intrinsic and extrinsic mechanisms. Intrinsic mechanisms comprise those referring to a lattice instability resulting in ferroelectric or relaxor-like behavior, coupled with a highly correlated electronic ground state. Contrary to other stoichiometric titanates, no ferroelectric transition has been observed in CCTO. Relaxor-like dynamical slowing down of dipolar fluctuations in nanosize domains has been proposed by Homes *et al.* from the optical conductivity measurements.[3] It has been argued that the high dielectric constant may arise from local dipole moments associated with off-center displacements of Ti atoms.[3] The structure does not exhibit a long range structural distortion, as typically observed in perovskite compounds. Within this model the absence of a structural phase transition is explained by the premise that the tilts of the TiO_6 octahedra are large enough to uncouple the local titanium distortions from each other, effectively decoupling the ferroelectric order parameter and the long-range crystal structure. The implications of this model could be tested experimentally using local structural probe, such as the atomic pair distribution function analysis (PDF). The off-center displacements of

Ti would imply large atomic displacement (thermal) parameters, and possibly octahedral tilt disorder.

Recently, Ramirez and collaborators suggested that local structural defects within the Ca-Cu sublattice of CCTO, if evidenced, may provide an intrinsic scenario for explaining the gigantic dielectric constant observed in this system.[7] In this view, the defects would disrupt an otherwise rigid Cu-O complex, and would be prone to *local* polarizability. However, since the defects are random, the polarization does not propagate over long range. According to the authors, significant diffuse scattering signal is expected in the high-dielectric-constant regime, with freezing at lower temperatures. Experimental verification of these predictions could also be performed by a local structural study such as EXAFS, or the PDF method that utilizes both Bragg and diffuse intensities.

Another possible explanation for the colossal dielectric properties of CCTO can be an extrinsic mechanism related to the microstructure of the sample, its morphology, and boundary layer effects.[8] Subramanian *et al.* argue that unusually high dielectric constant of CCTO is due to its microstructure because of the creation of an effective circuit of parallel capacitors as found in boundary-layer dielectrics.[1] Recent X-ray diffraction study on CCTO single crystals showed twinning on a fine scale in the microstructure of CCTO.[9] Twin boundaries are proposed to act in a manner to create a barrier layer capacitance, the effect known to produce extremely high dielectric constants. Sinclair *et al.* attribute the giant dielectric phenomenon to a grain boundary barrier layer capacitance.[10] The model features semiconducting perovskite grains with thin, insulating grain boundaries. The colossal dielectric constant has also been discussed to possibly originate from Maxwell-Wagner type contributions of depletion layers at the interface between sample and contacts or at grain boundaries, as has quite impressively been demonstrated on a variety of different materials.[11]

In order to assess the validity of various explanations for the giant dielectric response of CCTO it is necessary to characterize not only the average crystal structure, but also the local structure. In this work local structural properties of the CCTO system are investigated as a function of temperature within a range from 50 K up to room temperature using atomic pair distribution function analysis of the powder diffraction data.[12,13,14]

II. EXPERIMENTAL

The $CaCu_3Ti_4O_{12}$ sample was prepared by conventional solid state methods. Stoichiometric amounts of $CaCO_3$ (Mallinckrodt, 99.95% purity), CuO (J.T. Baker, 99.9% purity), and TiO_2 (EM Science, 99.7% purity) were weighed and mixed intimately using acetone in an agate mortar and pestle. The reaction mixture was preheated in a high form alumina crucible at 900°C for 8 hours. The preheated powder was reground and pressed into pellets. The pellets were heated in the presence of air at 1075°C for 24 hours. Purity of the final product was confirmed by x-ray powder diffraction using a Bruker D8 Advance diffractometer equipped with an incident beam Ge monochromator and a Braun position sensitive detector.

We performed a complementary neutron diffraction and x-ray diffraction study on powder samples of $CaCu_3Ti_4O_{12}$. Time-of-flight neutron diffraction experiments were carried out at Special Environment Powder Diffractometer (SEPD) at the Intense Pulsed Neutron Source (IPNS) at Argonne National Laboratory. About 10 g of polycrystalline sample was sealed in a cylindrical vanadium tube with He exchange gas. The sample was cooled using a closed-cycle He refrigerator, and data collected at 50 K, 100 K, 150 K, 200 K and 290 K. X-ray diffraction data were collected at X7A beamline of the National Synchrotron Light Source (NSLS) at Brookhaven National Laboratory. The sample was carefully packed between Kapton foils to avoid texture formation, and mounted within a closed cycle helium refrigerator. Data were collected at 50 K and 300 K in symmetric transmission geometry using 29.08 keV synchrotron radiation ($\lambda = 0.4257$ Å). Scattered radiation was collected with an intrinsic germanium detector connected to a multichannel analyzer. Several runs were conducted and the resulting X-ray diffraction patterns were averaged to improve the statistical accuracy and reduce any systematic effect due to instabilities in the experimental setup. The raw data were background-subtracted, corrected for flux and experimental effects such as sample absorption and multiple scattering, and normalized.[14]

From the normalized data the total scattering structure function, $S(Q)$,[12] is obtained, where $Q = |\mathbf{Q}| = |\mathbf{k} - \mathbf{k_0}|$ represents momentum transfer (magnitude of the scattering vector). The PDF function, $G(r)$, is then obtained by a Fourier transformation according to

$$G(r) = \frac{2}{\pi} \int_0^\infty Q[S(Q) - 1] \sin(Qr)\, dQ. \qquad (1)$$

The strength of the PDF technique is that it takes into account both Bragg and diffuse scattering components, and yields structural information on both long-range order and local structural disorder in materials. The function $G(r)$ gives the number of atoms in a spherical shell of unit thickness at a distance r from a reference atom. It peaks at characteristic distances separating pairs of atoms and thus reflects the atomic structure.[14] Neutron diffraction data processing was performed using PDFgetN analysis program package.[15] The neutron PDFs examined in this paper use data over a wide momentum transfer range, and were terminated at $Q_{max} = 28$ Å^{-1}. X-ray diffraction data were processed with help of the programs RAD[16] and IFO.[17] The X-ray diffraction PDFs investigated here use data up to $Q_{max} = 24$ Å^{-1}.

Data have been analyzed using the Rietveld method performed by GSAS program.[18] Structural information is obtained from the PDF data through a modeling pro-

cedure similar to the Rietveld method. However, it is carried out in *real-space* and yields the *local* structure rather than the average crystal structure.[14] From the refinements, different structural information can be extracted, such as lattice parameters, average atomic positions and amplitudes of their thermal motion, atomic displacements, and magnitudes of local octahedral tilts. The results reported here are obtained using the PDFFIT modeling program.[19] In cases where the average and local structure are the same (i.e., well-ordered crystals) the structural parameters obtained from Rietveld and the PDF are the same.[20] However, when the local structure deviates from the average structure the parameters from the PDF will reflect the local structure and the Rietveld parameters the periodically averaged values.

III. RESULTS

First we compare our results with published structural data. Several studies of the average crystalline structure exist.[1,2,4,9] None of these studies finds evidence of a structural distortion as a function of temperature or pressure that would couple to the dielectric properties.[7] Despite the possible importance of the lattice, these structural studies are not thorough; either being derived solely from x-ray data (and therefore rather insensitive to important oxygen structural parameters) or presenting a sparse set of data points. In addition, a systematic temperature dependent local structural study has not been performed, to date. Local structure has only been investigated in related $CaCu_3Ru_4O_{12}$, and in a different context.[21] Here we present a joint x-ray and neutron diffraction study where the data are analyzed both in real and reciprocal space.

Typical Rietveld fits of the X-ray diffraction data are shown in Fig. 2. The data are well explained within the $Im\overline{3}$ space group at both low and high temperature, confirming the absence of phase transitions and distortions in the average structure, in quantitative agreement with earlier results.[1]

Typical PDFs of CCTO both from neutron diffraction and X-ray diffraction experiments are shown in Fig. 3. It should be noted that *neutron* PDFs of CCTO exhibit peculiar behavior: contributions of Ti-O and Cu-O to the first PDF peak cancel out, so that the first peak is 'missing'. This is due to the negative scattering length of Ti for neutrons, and due to the almost identical Ti-O and Cu-O distances. This perfect cancellation of the Cu-O and Ti-O intensities (e.g. compare Fig. 3 (a), (b) and (c) at $r = 1.9$ Å) will only occur for selected peaks in the structure. Other peaks contain information about the relative positions of these ions and so a refinement over a wide-range of r-will provide accurate structural information on these species.

Structural modeling of the CCTO PDF profiles was performed observing constraints of the $Im\overline{3}$ symmetry. Structural parameters are summarized in Table I. The

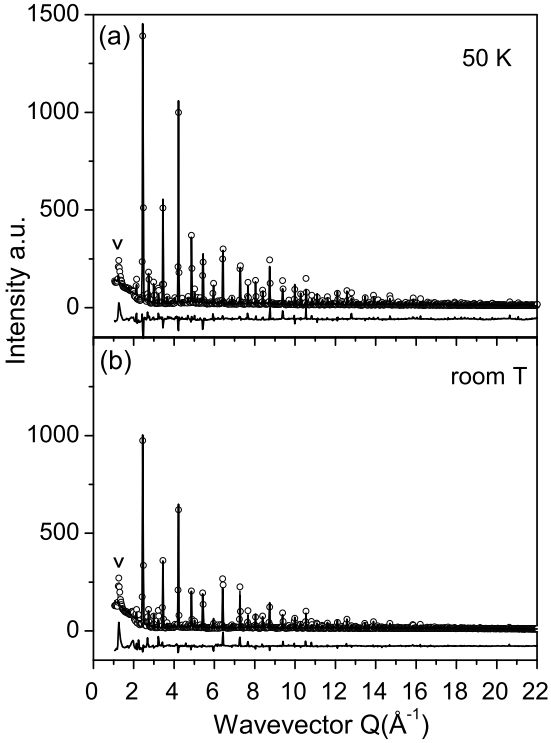


FIG. 2: Experimental (open circles) and Rietveld fitted X-ray diffraction patterns (solid line) of $CaCu_3Ti_4O_{12}$ at (a) 50 K and (b) room temperature. The residual difference is given in the bottom part of each panel. The broad peak at very low Q-values (marked with V) originates from the sample environment (aluminum shroud of the displex cooling system).

TABLE I: Results of the neutron powder diffraction structural study of CCTO, observing $Im\overline{3}$ space group constraints: lattice parameter and atomic coordinates. The atomic positions are Ca(0,0,0), Cu(0,0.5,0.5), Ti(0.25,0.25,0.25), O(x,y,0). Numbers in parentheses are expected standard deviations obtained from fitting.

T (K)	a (Å)	x(O)	y(O)
50	7.3818(5)	0.3029(1)	0.1790(1)
100	7.3823(5)	0.3029(1)	0.1789(1)
150	7.3836(5)	0.3031(1)	0.1790(1)
200	7.3856(5)	0.3031(1)	0.1791(1)
290	7.3906(5)	0.3032(1)	0.1792(1)

lattice parameter shows the expected temperature dependence. Corresponding isotropic displacement parameters, $U_{iso} \equiv \langle u^2_{iso} \rangle$ in standard notation, are listed in Table II. Nearest neighbor distances are shown in Fig. 4: while Ca-O (solid triangles) and Ti-O (solid squares) distances decrease monotonically with decrease in temperature, Cu-O distance (sold circles) appears to be temperature independent, reflecting the rigidity of the square-planar coordination of Cu sublattice. Rietveld obtained

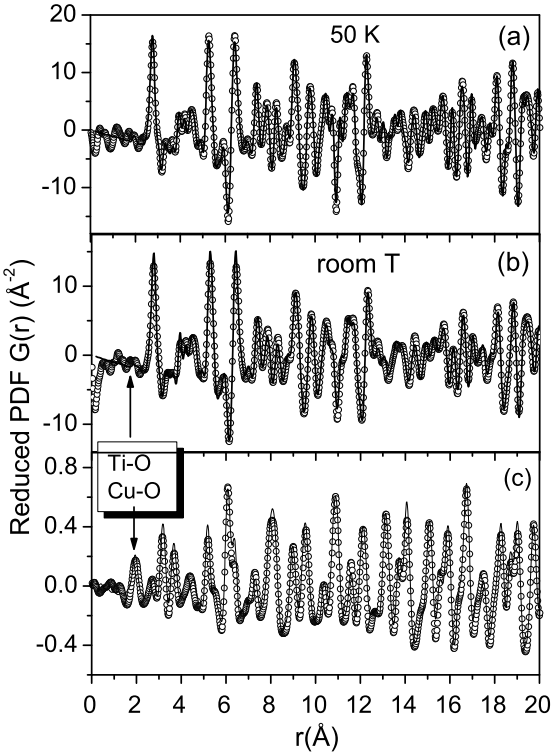


FIG. 3: Reduced atomic PDF of CCTO. Experimental data (open circles) and fits (solid lines) shown for: (a) data obtained from neutron diffraction at 50 K and (b) at room temperature; (c) data obtained from X-ray diffraction at room temperature. Goodness of the PDF fit is around 15%. The PDF profiles corresponding to the two probes have different intensity distributions, reflecting different scattering properties of the sample for neutron diffraction and X-ray diffraction. Arrows mark the nearest neighbor PDF peak: in CCTO it contains two contributions, coming from Ti-O and Cu-O distances (see text).

TABLE II: Isotropic displacement parameters, U_{iso}, in units of Å^2, as obtained from PDF structural refinements of neutron powder diffraction data. Numbers in parentheses are standard deviations estimated from fitting.

T (K)	Ca	Cu	Ti	O
50	0.0041(2)	0.0027(2)	0.0028(2)	0.0034(2)
100	0.0048(2)	0.0028(2)	0.0032(2)	0.0038(2)
150	0.0055(2)	0.0033(2)	0.0034(2)	0.0040(2)
200	0.0060(2)	0.0042(2)	0.0039(2)	0.0043(2)
290	0.0057(2)	0.0056(2)	0.0047(2)	0.0050(2)

distances (not shown) are in agreement with PDF, within the experimental uncertainties. The distances at room temperature are in good agreement with those reported in Ref. 4, but differ somewhat from those reported in Ref. 1 where the temperature dependence of the Cu-O bond lengths appears to be over estimated.

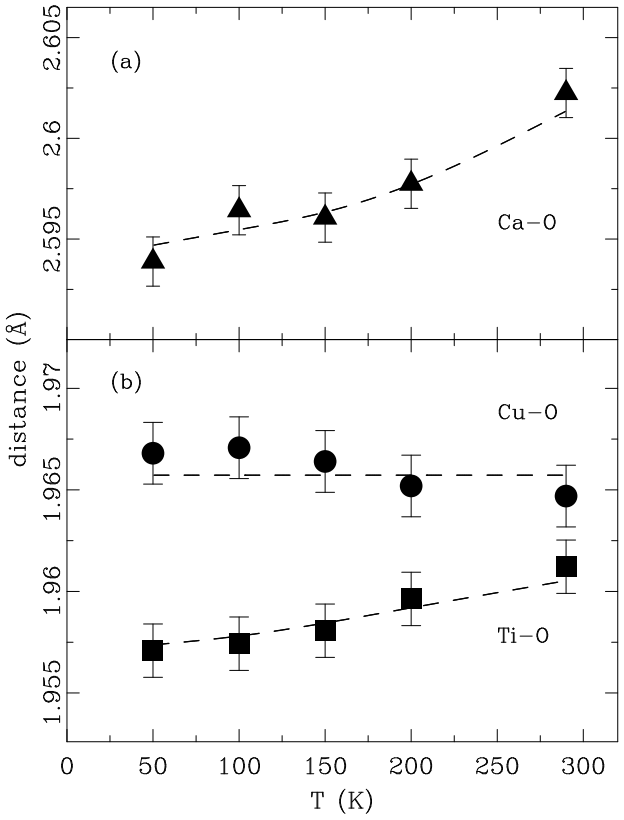


FIG. 4: Temperature dependence of the nearest neighbor distances in $CaCu_3Ti_4O_{12}$: (a) Ca-O (solid triangles), (b) Cu-O (solid circles) and Ti-O (solid squares). Dashed lines are guides for the eye.

The results of the polyhedral analysis revealed very small changes in the volumes and shapes of TiO_6 octahedra on cooling from room temperature down to 50 K. Changes in the magnitude of the octahedral tilting, as expressed by the Ti-O-Ti angle, are smaller than 0.3° (less than 0.2% change).

IV. DISCUSSION

A. Evidence for non-Debye local atomic displacements

Inspection of the PDF displacement parameters, that provide clues on local disorder, revealed an unusual temperature dependence of the isotropic displacement parameter of calcium. At low temperature it is 50% larger than the corresponding value for copper. However, at room temperature the two appear to be equal (Fig. 5). We should note that this observed behavior relies on a single high-temperature data-point. We are in the process of extending our data collection in this region to confirm this result and extract in greater detail the temperature dependence of this parameter.

TABLE III: Estimate of the Debye temperature, θ_D, and static offset parameter, σ^2_{off}, for various constituent atoms of CCTO. Parameters are obtained by fitting Debye model to the temperature dependencies of the PDF displacement amplitudes.

Atom	Θ_D (K)	σ^2_{off} (Å^2)
Ca	450(20)	0.0021(1)
Cu	360(20)	0.0004(9)
Ti	545(20)	0.0014(2)
O	923(20)	0.0011(1)

The data have been fit with a Debye model to understand whether or not the low-temperature displacement factors are anomalous.[22,23,24] Two-parameter fitting of the Debye curve to the displacement parameter temperature dependencies has been carried out, using

$$\sigma_D^2 = \frac{3\hbar^2}{mk_B\Theta_D}\left[\frac{1}{4} + \left(\frac{T}{\Theta_D}\right)^2 \int_0^{\frac{\Theta_D}{T}} \frac{x}{e^x - 1}dx\right] + \sigma^2_{off}, \quad (2)$$

where the parameters are the Debye temperature, Θ_D, and the static offset, σ^2_{off}. Results of the fitting are summarized in Table III and shown in Fig. 5.

Oxygen and Ti parameters exhibit the expected behavior with relatively high Debye temperatures and small offsets. The fits are shown in Fig. 5(b). The large Debye temperature of oxygen is similar to that obtained in cubic manganites.[20] The Debye parameters for Ti are also similar to perovskite titanates such as $BaTiO_3$.[25] There is, therefore, no evidence for local disorder on the titanium or oxygen sublattices. This suggests that nanoscale tilt disorder, as envisioned by Ramirez *et al.*[7] to explain colossal dielectric behavior, is not present.

The Ca and Cu parameters behave more interestingly. The atomic displacement parameter associated with the Ca sites remains unusually large at low temperature (50% higher than that of Cu) with a significant offset parameter. This may suggest local static displacive disorder on this site, with a magnitude of approximately 0.05 Å. This will be discussed later in terms of bond-valence sum predictions for the Ca site. We also note that all the points except the high temperature one are well explained by the fit. The dashed line in Fig. 5(a) is the same Debye curve of Ca, but with the offset parameter *set to zero*. It is interesting to note that the high temperature U_{iso}(Ca) point lies on the dashed curve where the static component is switched off. This observation may be suggestive of a crossover from a disordered state at low temperature to a more ordered state at high temperature, with crossover temperature in the 200-300 K range. Further measurements to verify this result are planned.

Also interesting is the low Debye temperature obtained for copper from the fitting. Copper is expected to be stiffly bonded to its four close oxygen neighbors and a much higher Debye temperature than the observed 360 K might be expected. It is also notable that the Debye fit (Fig. 5(a) lower solid line) fails at low temperature for the copper site with the low-temperature data-point displaced upwards from the Debye curve. A possible explanation is that the actual Debye temperature of the copper is actually higher than indicated by the fit. This would give a flatter Debye curve and explain the low-T behavior, as indicated by a thick dotted line in Fig. 5(a) corresponding to a Debye temperature of 785 K. In this picture, above 100 K an additional non-Debye but T-dependent excess disorder appears on this site.

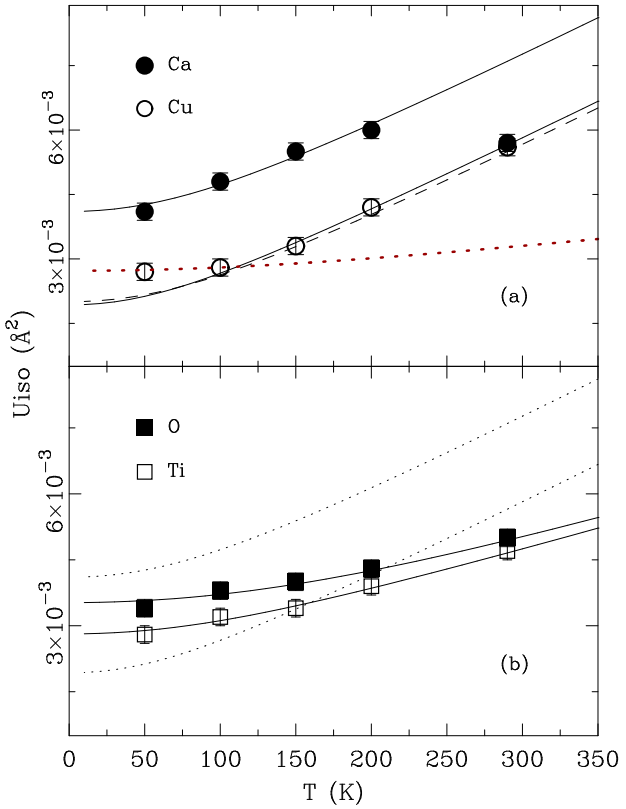


FIG. 5: (a) Evolution with temperature of the isotropic displacement parameters of Ca and Cu. Solid lines are from the Debye model for Ca and Cu, with parameters as specified in Table III. Dashed line is a Debye curve of Ca corresponding to the same Debye temperature, but with offset parameter set to zero (see text). Thick dotted line is a Debye model for Cu using higher Debye temperature of 785 K. (b) Isotropic displacement parameters of Ti and O as a function of temperature, with Debye model curves superimposed (solid lines). Debye model curves for Ca and Cu (dotted lines) are also shown for comparison.

B. Bond valence sum prediction of the crystal structure of CCTO

Here we discuss bond valence sum calculations that make predictions about the stability as a function of temperature of the observed perovskite structure. These may indicate a tendency to local structural distortions that

are prevented from propagating by the bracing described above.

Normally in an ABO_3 perovskite (*i.e.* $CaTiO_3$) the octahedral tilting distortion increases as the temperature decreases. This occurs because the A-O bonds contract more rapidly in response to the decreasing temperature than the B-O bonds. However, in CCTO the situation is somewhat different. Firstly, the Cu-O bond length is very sensitive to changes in the magnitude of the tilting distortion, whereas the Ca-O bond length contracts much more slowly with increasing tilt. Secondly, the Cu-O bonds are considerably more covalent than the typical A-O bond, and exhibit relatively little thermal expansion over the temperature range examined in this study, as shown in Fig. 4. These considerations help to explain why both the tilt magnitude and the Cu-O distance are essentially independent of temperature.

As described above, the Cu-O bonding locks-in the tilting at what is essentially a constant value. However, the optimal Ca-O bond length should still contract fairly substantially with decreasing temperature, as it would in a typical perovskite such as $CaTiO_3$. Consequently, there will be a crossover temperature where the Ca-O and Cu-O bonding are perfectly matched. Above this temperature the calcium will be overbonded. That is to say that the effective size of Ca will be too large for its environment and the Ca-O bonds will be in compression. Below the optimal temperature the calcium will be underbonded, so that the effective size of Ca is too small for its environment and the Ca-O bonds will be in tension. In order to estimate the optimal temperature for CCTO we have utilized the structure prediction capabilities of the SPuDS software package[26] to evaluate the competition between Cu-O, Ca-O and Ti-O bonding as a function of temperature. SPuDS is based on the bond valence concept[27,28] and has been shown to be quite accurate in predicting the magnitude of octahedral tilting distortions in perovskites.[26] The thermal expansion of all bonds was assumed to be inversely related to the valence of the bond as suggested by Brown.[29] Figure 6 shows the predicted Ti-O-Ti angles as a function of temperature for $CaCu_3Ti_4O_{12}$ and $CaTiO_3$. In agreement with the experimental results reported here the temperature dependence of the tilting in CCTO is predicted to be much smaller than that of $CaTiO_3$. The predicted calcium and copper bond valence sums, as well as the global instability index (GII),[30] are shown in Fig. 7 as a function of temperature. The global instability index reaches a minimum near 260 K, where the bonding requirements of calcium and copper are optimally matched. Below this temperature the Ca atoms become underbonded and the copper atoms overbonded. Even though this method of estimating the crossover temperature is fairly crude it is interesting to note that what seems to be a crossover in the Ca isotropic displacement parameter takes place near this temperature.

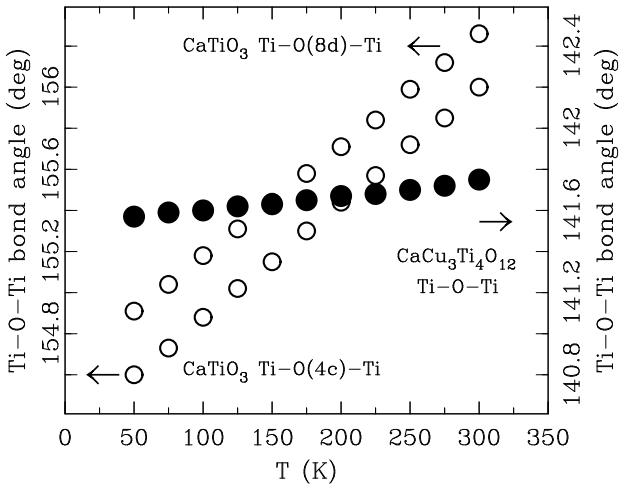


FIG. 6: Expected Ti-O-Ti bond angles as a function of temperature for $CaCu_3Ti_4O_{12}$ and $CaTiO_3$ from bond valence analysis.

C. Local structure and braced lattice model

Despite the large tilting of TiO_6 octahedra in CCTO, no structural phase transition to a lower symmetry phase, as observed in related $CaTiO_3$, $SrTiO_3$ and $BaTiO_3$,[25,31,32] is evident. These transitions typically occur because underbonded ions (i.e., ions that are too small for their coordination environment) desire to lower their site symmetry. This should be observed in the current case, because Ca is in this underbonded state at low temperature. However, no symmetry lowering phase transitions are observed. This has recently been argued to be due to the bracing of the perovskite structure by the Cu-O square complex preserving the cubic structure of CCTO at all temperatures.[7] Distorting the Cu-O bonds is energy expensive, and this prevents changes in TiO_6 octahedral tilting, as such changes would affect the copper coordination by changing its oxygen-square environment. Rigidity of the Cu-O complex is evident from the temperature independence of the Cu-O nearest neighbor distance (Fig. 4 (b)). Our displacement parameter results described above suggest that it is plausible that off-center displacements of Ca may be present in the structure that are not long-range ordered and do not result in a phase transition.

Ramirez and collaborators investigated, within the mean-field approximation, a possibility of having isolated polarizable defects in otherwise ideal CCTO structure.[7] It is speculated that the defects are either Cu vacancies or interchange of Ca and Cu sites in such a manner that the rigid square Cu-O network, bracing the structure, is *locally* disrupted. This local absence of bracing would, according to this scenario, allow for local, short-range ordered, distortions to take place. The lack of average structural evidence is argued to be due to the low concentration of defect sites, as well as due to the

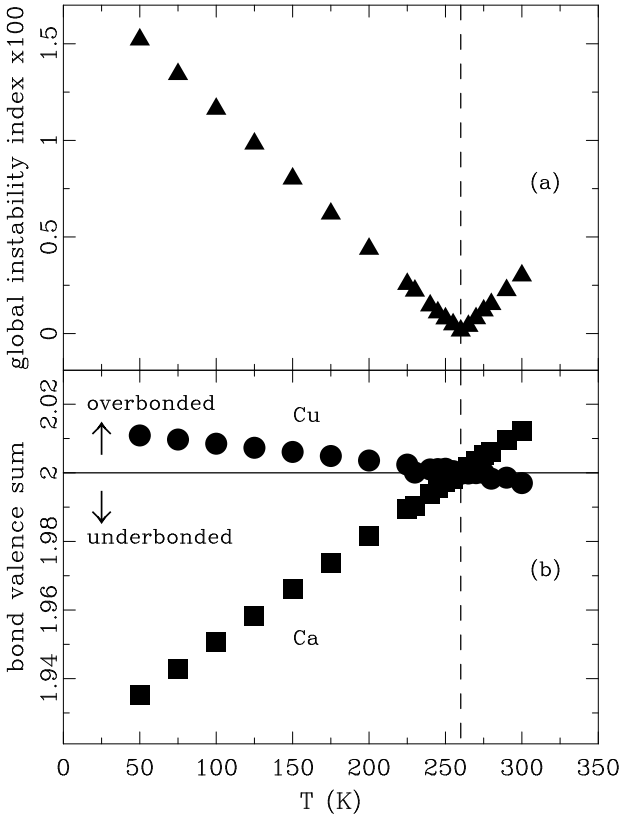


FIG. 7: (a) Global instability index (GII) as a function of temperature, calculated for $CaCu_3Ti_4O_{12}$. (b) Predicted bond valence sums for Ca and Cu. Solid line denotes optimal valence for the two atomic types, while dashed line marks minimum of the GII where the bonding requirements of Ca and Cu are optimally matched.

relaxation between alternative equivalent configurations that would preserve the average cubic structure. It is then expected that a diffuse scattering signal in neutron scattering experiments would be observable in the large-dielectric-constant regime. Polyhedral analysis, as mentioned above, does not reveal changes in the octahedral size, shape, and rotation in the local structure of CCTO. This argues against locally correlated distortions of the octahedral network. On the other hand, we do see evidence for possible disorder on the Ca and Cu sublattices that may be locally correlated. Observing possible local correlations in Ca displacements is beyond the accuracy of our measurement.

Such polarizable defects, embedded into a background with dielectric constant ϵ_0 and relaxing at a rate determined by temperature and an energy barrier separating alternative configurations, are proposed to have small concentration, of the order of 10^{-3}. The detection of defects at this level is beyond our measurements. However, the idea that locally interrupted bracing due to these defects would allow for local distortions involving TiO_6 units to take place is inconsistent with the PDF results, and also the results of recent polarized Raman study on single-crystal CCTO and within broad temperature range.[33] Therefore, local octahedral tilting distortions can be clearly ruled out as a candidate for the observed large dielectric constant.

D. Implications for dielectric properties

We address possible implications of the disorder on Ca and Cu sublattices for the dielectric properties of CCTO. Although there is now mounting evidence that the unusual dielectric properties of CCTO may be extrinsic in nature,[9,11] the possibility for an intrinsic mechanism is not completely ruled out.[7] Even with an extrinsic mechanism the question remains what is special about CCTO and why is such dielectric behavior not much more widely observed. One of the remaining plausible avenues for the intrinsic mechanism involves a system that is at the edge of the Clausius-Mossotti catastrophe.[11] Origin of the giantic dielectric constant in the low-frequency mode and also unusually large dielectric constant in the high-frequency regime (of the order of 100), as well as the exact nature of the switching mechanism between these two are not clearly understood.

The defect-model in Ref. 7 describes a system involving a small concentration of polarizable defects, with a temperature independent polarization, embedded in a background dielectric constant, ϵ_0. The enormous real part of the dielectric constant of such a system is then readily achieved providing (i) $\epsilon_0 \gg 1$, (ii) the polarizability of the defects is of the order of their volume, and (iii) the concentration of the defects is reasonably small, $\ll 1$. This model appears to capture rather nicely the unusually high value of the measured dielectric constant plateau of the order of 5000.[7] However, sensitivity of the dielectric constant plateau value, within this model, to the exact value of ϵ_0 used is remarkable. Changing ϵ_0 from 100 to about 70, and keeping all other parameters in the model the same, changes the plateau value from about 5128 to only about 223. This demonstrates the importance of the background dielectric constant within this model.

Study of the optical properties of CCTO[3] reveals an unusual temperature dependence of the real part of the dielectric function in the far-infrared (FIR) limit ($\omega \leq 20$ cm^{-1}) , ϵ_{FIR}. This is found to change from ~ 70 at high temperature, to ~ 120 at base temperature, an increase of about 70%. The order of ϵ_{FIR} was concluded to be in good agreement with the high frequency limit (and low temperature) value of the measured dielectric constant of CCTO, presumably ϵ_0 featured in the defect-model. The increase in the FIR value of the dielectric constant has an onset temperature of the order of 200 K, and its temperature dependence has been assigned to the violation of the f-sum rule and the increase of the oscillator strengths of the IR modes. This onset temperature seems to correlate well with the onset temperature of the local

static disorder on Ca sublattice observed from the PDF analysis.

While the issues addressed here are far from being resolved, we speculate that Ca sublattice may play a key-role in explaining some of the observed properties of CCTO. Distribution of the Ca atoms between displaced lattice sites in some sort of multi-well potential at low temperatures may provide a natural explanation for the observed enlarged thermal amplitudes. Furthermore, if this happens in a *locally* correlated fashion, within some sort of nanodomain structure, it could possibly be relevant for the anomalous increase of far-infrared ϵ_{FIR} observed in studies of the optical properties.[3] In this view, upon increasing temperature, the local order on Ca sites is destroyed, and this leads to the decrease of the intrinsic (high frequency) dielectric constant. Small volume fraction polarizable defects, be they intrinsic or extrinsic, would then give the required amplification of the low-frequency dielectric constant through the mechanism described in Ref. 7.

V. SUMMARY

Local structural properties of the CCTO system are investigated as a function of temperature within a range from 50 K up to room temperature. Data were analyzed using Rietveld refinement and the atomic pair distribution function (PDF) analysis of the powder diffraction data has been employed to extract the local structural information. In agreement with earlier studies, no signature of a phase change has been observed. The temperature dependence of the nearest neighbor Cu-O distance is very flat, supporting the idea that this is bracing the structure. No evidence for perovskite-type local distortions is found. The isotropic Ca displacement parameter has a significant static offset compared to the expected Debye behavior. It also appears to behave anomalously at high-temperature, though this needs to be verified by more measurements. The Debye temperature of copper is surprisingly low, given its covalently bonded nature. We note that the T-dependence of the Cu displacement parameters could be reconciled with a higher Debye temperature coupled with non-Debye but temperature dependent displacements, where these extra displacements begin appearing above ~ 100 K.

Simple modeling based on bond valence concepts supports the local structural observations. The temperature at which both the Ca and Cu environments are optimal has been estimated to be in the vicinity of 260 K. At lower temperatures the Ca becomes underbonded. This may result in an off-center displacement of Ca ions. If these displacements cannot become long-range ordered because of the braced structure, this might explain the absence of a structural phase transition and the static offset of the Ca thermal parameters.

Local domains of coherently polarized displaced Ca ions could possibly exist at low temperature and may be related to the enhanced values of far-IR dielectric constant, a parameter playing an important role in intrinsic-mechanism models for the large dielectric response at the edge of dielectric catastrophe, such as that proposed by Ramirez *et al.*[7]. This model seems capable of explaining the large dielectric constants; however, it is very sensitive to the exact value of the background far-IR dielectric response of the material that provides an amplification effect. From this study we cannot say whether such an intrinsic mechanism, or an extrinsic mechanism, is responsible for the colossal dielectric behavior.

VI. ACKNOWLEDGEMENTS

We are thankful to Simine Short for providing valuable help with the neutron diffraction data collection. We would like to thank Mike Lufaso for his development of the program SPuDS. This work was supported financially by DOE-BES through grant FG02-97ER45651. The experimental data were collected on X7A beamline at the NSLS at Brookhaven National Laboratory, and on SEPD at the IPNS at Argonne National Laboratory. NSLS is funded by the US Department of Energy under contract DE-AC02-98CH10886. IPNS is funded by the US Department of Energy under contract W-31-109-ENG-38.

[1] M. A. Subramanian, D. Li, N. Duan, B. A. Reisner, and A. W. Sleight, J. Solid State Chem. **151**, 323 (2000).
[2] A. P. Ramirez, M. A. Subramanian, M. Gardel, G. Blumberg, D. Li, T. Vogt, and S. Shapiro, Solid State Commun. **115**, 217 (2000).
[3] C. C. Homes, T. Vogt, S. M. Shapiro, S. Wakimoto, and A. P. Ramirez, Science **293**, 673 (2001).
[4] B. Bochu, M. N. Deschizeaux, J. C. Joubert, A. Collomb, J. Chenavas, and M. Marezio, J. Solid State Chem. **29**, 291 (1979).
[5] A. M. Glazer, Acta Crystallogr. B **28**, 3384 (1972).
[6] A. Koitzsch, G. Blumberg, A. Gozar, B. Dennis, A. P. Ramirez, S. Trebst, and S. Wakimoto, Phys. Rev. B **65**, 052406 (2002).
[7] A. P. Ramirez, G. Lawes, V. Butko, M. A. Subramanian, and C. M. Varma, cond-mat/0209498.
[8] L. He, J. B. Neaton, M. H. Cohen, D. Vanderbilt, and C. C. Homes, Phys. Rev. B **65**, 214112 (2002).
[9] M. A. Subramanian and A. W. Sleight, Solid State Sci. **4**, 347 (2002).
[10] D. C. Sinclair, T. B. Adams, F. D. Morrison, and A. R. West, Appl. Phys. Lett. **80**, 2153 (2002).
[11] P. Lunkenheimer, V. Bobnar, A. V. Pronin, A. I. Ritus, A. A. Volkov, and A. Loidl, Phys. Rev. B **66**, 052105 (2002).
[12] B. E. Warren, *X-Ray Diffraction*, Dover, New York, 1990.

[13] T. Egami, Mater. Trans. **31**, 163 (1990).
[14] S. J. L. Billinge, in *Local Structure from Diffraction*, edited by S. J. L. Billinge and M. F. Thorpe, page 137, New York, 1998, Plenum.
[15] P. F. Peterson, M. Gutmann, Th. Proffen, and S. J. L. Billinge, J. Appl. Cryst. **33**, 1192 (2000).
[16] V. Petkov, J. Appl. Cryst. **22**, 387 (1989).
[17] V. Petkov and R. Danev, J. Appl. Cryst. **31**, 609 (1998).
[18] A. C. Larson and R. B. Von Dreele, Report No. LAUR-86-748, Los Alamos National Laboratory (1994).
[19] Th. Proffen and S. J. L. Billinge, J. Appl. Cryst. **32**, 572 (1999).
[20] Th. Proffen, R. G. DiFrancesco, S. J. L. Billinge, E. L. Brosha, and G. H. Kwei, Phys. Rev. B **60**, 9973 (1999).
[21] S. G. Ebbinghaus, A. Weidenkaff, and R. J. Cava, Solid State Commun. **167**, 126 (2002).
[22] C. Kittel, *Quantum Theory of Solids*, John Wiley, New York, 1963.
[23] G. Beni and P. M. Platzman, Phys. Rev. B **14**, 1514 (1976).
[24] I.-K. Jeong, R. H. Heffner, M. J. Graf, and S. J. L. Billinge, cond-mat/0209603.
[25] G. H. Kwei, A. C. Lawson, S. J. L. Billinge, and S.-W. Cheong, J. Phys. Chem. **97**, 2368 (1993).
[26] M. W. Lufaso and P. M. Woodward, Acta Crystallogr. B **57**, 725 (2001).
[27] I. D. Brown, Chem. Soc. Rev. **7**, 359 (1978).
[28] I. D. Brown and D. Altermatt, Acta Crystallogr. B **41**, 244 (1985).
[29] I. D. Brown, A. Dabkowski, and A. McCleary, Acta Crystallogr. B **53**, 750 (1997).
[30] A. Salinas-Sanchez, J. L. Garcia-Munoz, J. Rodriguez-Carvajal, R. Saez-Puche, and J. L. Martinez, J. Solid State Chem. **100**, 201 (1992).
[31] S. A. T. Redfern, J. Phys.: Condens. Matter **8**, 8267 (1996).
[32] K. Tsuda and M. Tanaka, Acta Crystallogr. A **51**, 7 (1995).
[33] N. Kolev, R. P. Bontchev, A. J. Jacobson, V. N. Popov, V. G. Hadjiev, A. P. Litvinchuk, and M. N. Iliev, Phys. Rev. B **66**, 132102 (2002).